



**HAL**  
open science

## A personalized path generation for an autonomous vehicle overtaking maneuver

Benoit Vigne, Rodolfo Orjuela, Jean-Philippe Lauffenburger, Michel Basset

### ► To cite this version:

Benoit Vigne, Rodolfo Orjuela, Jean-Philippe Lauffenburger, Michel Basset. A personalized path generation for an autonomous vehicle overtaking maneuver. 11th IFAC Symposium on Intelligent Autonomous Vehicles - IAV2022, Jul 2022, Prague, Czech Republic. hal-03720989

**HAL Id: hal-03720989**

**<https://hal.science/hal-03720989>**

Submitted on 12 Jul 2022

**HAL** is a multi-disciplinary open access archive for the deposit and dissemination of scientific research documents, whether they are published or not. The documents may come from teaching and research institutions in France or abroad, or from public or private research centers.

L'archive ouverte pluridisciplinaire **HAL**, est destinée au dépôt et à la diffusion de documents scientifiques de niveau recherche, publiés ou non, émanant des établissements d'enseignement et de recherche français ou étrangers, des laboratoires publics ou privés.

# A personalized path generation for an autonomous vehicle overtaking maneuver

Benoit Vigne, Rodolfo Orjuela, Jean-Philippe Lauffenburger,  
Michel Basset

*Université de Haute-Alsace, IRIMAS UR7499, Mulhouse, France  
(e-mail: firstname.name@uha.fr).*

---

**Abstract:** The acceptability by a population for new technology is conditioned by its benefits and its adaptability. While an autonomous vehicle could be a nice solution as an intelligent transportation system to decrease road crashes, traffic jams, etc., the choice of a driving style (relaxed/sporty) could be a good factor of adaptability. This study presents a method to optimize a local overtaking trajectory defined as a sigmoid function integrating constraints of comfort, safety, and path continuity. An only one driving style parameter allows obtaining different paths from smooth to tight shapes respecting previous constraints. Simulations of use cases show good performance of the developed algorithm.

*Keywords:* autonomous vehicle, driving style, parameter optimization, overtaking maneuver

---

## 1. INTRODUCTION

In the last decade, research on path planning focused on generating optimal paths with a predetermined metric consisting in distance, jerk, fuel consumption, maximum speed and minimized time. The most common methods are classified into six families: Graph search methods (A\*, Dijkstra algorithms), sampling-based planners (Rapidly-exploring Random Tree algorithm), artificial potential fields, interpolating curves planners (clothoid, spline, Bezier, polynomial, sigmoid), numerical optimization (Model Predictive Control) and artificial intelligence (fuzzy logic, Recurrent Neural Network). This list is non-exhaustive and methods can be mixed. All have strengths and limits, reviewed in details in Gonzalez et al. (2016) and Claussmann et al. (2020).

As these methods have now reached maturity, passenger comfort is emerging as an additional criterion and several solutions - including those mentioned above - have been proposed to improve driving comfort. One consists in limiting the forces acting on the car and its passengers. Longitudinal and lateral forces stem respectively from accelerating/braking action and steering. Logically limiting longitudinal and lateral jerks as well as acceleration results in smoother vehicle motion (González et al., 2016). Another method aims at generating human-like paths minimizing steering control discontinuity and smoothness. Clothoid curves with continued curvature is well suited and is already used for road and railway design (Alia et al., 2015). However, their complexity to draw limits its use for real-time applications.

Path personalization requires to adapt passenger parameters of the path planner and decision making modules to mimic human driving style. Two approaches are used in the literature: the first one is explicit since the user has to fit himself his/her ride comfort wishes. In Bae et al. (2020) a full scale from cautious to aggressive is used to determine thresholds for both longitudinal and lateral acceleration

and jerk used by an optimal motion planning algorithm. The second one is implicit and involves a learning phase to estimate driving parameters. In Huang et al. (2021), multi-dimensional time series regression allows the calibration of longitudinal and lateral models of lane change maneuvers. Only the implicit approach makes it possible to fine tune the model according to a typical parameter such as relaxed or sporty driving style. However, the learning process may take time and might not be able to be adapted to a shared Autonomous Vehicle (AV) service.

Most often, comfortable and sporty driving style can be considered antagonistic. The comfortable style is synonymous of a smooth path while the sporty style is associated to a tight path. This feature is particularly true in the overtaking process with two lane change maneuvers with one decision making process. In this paper we defined and merged criteria for both styles, to optimize a local trajectory under constraints while ensuring a continuous comfort profile adaptation through an explicit parameter. Moreover, we successfully used the sigmoid function with parameters based on vehicle dynamic and geometric constraints. This guarantees the feasibility of generating smooth to tight path shapes without discontinuity while ensuring lateral stability.

The rest of this paper is organized as follows. Section 2 describes the problem formulation, including the work assumptions and the studied driving maneuver. Section 3 reports the overall optimization method and its adaptation to the overtaking maneuver, path generation is presented in Section 4. Section 5 describes the validation process and results are discussed. Finally, Section 6 draws some conclusions and highlights some perspectives.

## 2. PROBLEM STATEMENT

One of the most challenging driving situation is the overtaking maneuver because of simultaneous control of both

lateral and longitudinal positions. Overtaking involves at least two vehicles driving at different speeds in the same direction and on the same lane. The ego vehicle (EV) is the controlled vehicle arriving behind the leader vehicle (LV) at a higher speed so that it has to overtake LV. As shown in Fig. 1, the maneuver can be split into three successive phases. In phase ①, after safety check, the decision making process triggers a local path generation to shift EV on its adjacent lane and bring it alongside LV. In phase ②, the two vehicles drive in parallel lanes at different speeds so that EV overtakes LV. This transition deals with a small lateral gap between vehicles and requires more attention. In the final phase ③, the decision-making process conditioned by safety can trigger a local path generation to bring EV back to the initial lane in front of LV.

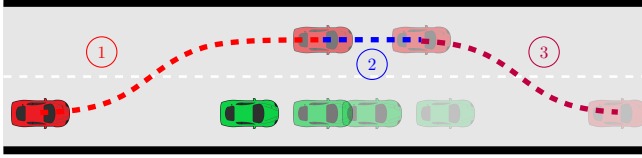


Fig. 1. Overtaking maneuver

In this context, the maneuver dependent on a double lane change could be affected by the driving style. We propose a method to generate personalized path from smooth to tight shapes respecting constraints of comfort, safety and continuity with only one parameter.

The maneuver description provides the framework of our study of local path planning. However, an overtaking maneuver also depends on additional vehicles neighboring both EV and LV. For instance, on the highway, vehicles on adjacent lanes can hinder pulling out to pass LV in front (phase ①), or vehicles in front of LV, can hamper the return phase (phase ③). On a rural road, the decision-making process must prohibit a frontal crash with a vehicle driving on the opposite lane. In such situations longitudinal speed must be adjusted and a complex decision-making process must be developed.

The present work focuses on the lateral motion only and restricts therefore the overtaking maneuver to a scenario meeting the three following conditions:

- EV and LV are locally the only vehicles.
- The speed of both vehicles is constant during the whole maneuver.
- The road is straight.

The first assumption allows focusing only on trajectory generation with a decision-making process reduced to the control of the lane change depending on the relative position of EV and LV. The second assumption reduces the trajectory generation to lateral path generation with constant speed profiles. The last one is safety-oriented and avoids dangerous overtaking maneuver in a curve. We acknowledge that making the maneuver conditional to these three assumptions may influence the driving style.

### 3. PROPOSED PARAMETERS OPTIMIZATION

In our case, the lateral deviation  $y$  is defined using a parametric function of the longitudinal position  $x$  and several parameters. This expression integrates comfort and

vehicle dynamics limits definitions and allows deducing optimal parameters for a safe lane change maneuver. Among the natural S shape curves (spline, hyperbolic tangent, etc.), sigmoid curves are popular due to the few parameters characterizing them (Ben-Messaoud et al., 2018).

#### 3.1 The sigmoid function

The overtaking local path can be defined through the sigmoid function:

$$y(x) = \frac{d_{lat}}{1 + e^{-\xi(x - \frac{d_{long}}{2} - b)}} \quad (1)$$

with 4 parameters having an impact on the curve shape. The lateral deviation  $d_{lat}$  is a constant dependent on the road width. The longitudinal stretching  $d_{long}$  is a constant dependent on the vehicle speed and the initial distance between EV et LV (see section 4). The two last parameters are  $\xi$ , the curvature form factor, and  $b$ , the spatial longitudinal delay.

To allow the sigmoid curve respecting both geometrical and vehicle dynamics constraints under personalized driving styles,  $\xi$  and  $b$  are bounded as demonstrated in Ammour et al. (2020):

$$\begin{cases} \xi_{min} < \xi < \xi_{max} \\ b_{min} < b < b_{max} \\ \text{with} \\ \xi_{min} = \frac{2}{d_{long} - 2b_{min}} \log\left(\frac{1 - y_{err}}{y_{err}}\right) \\ \xi_{max} = \sqrt{\frac{\rho_{max}(\gamma + 1)^3}{d_{lat}^2 \gamma(\gamma - 1)}} \\ b_{min} = 0 \\ b_{max} = \frac{d_{long}}{2} - \frac{1}{\xi_{max}} \log\left(\frac{1 - y_{err}}{y_{err}}\right) \end{cases} \quad (2)$$

where  $\gamma = e^{1.3170}$ ,  $y_{err}$  the relative error on the curve extremities, and  $\rho_{max} = \frac{a_{y_{max}}}{v_x^2}$  the maximum curvature defined by Rajamani (2012),  $a_{y_{max}}$  being the maximum desired lateral acceleration and  $v_x$  the vehicle longitudinal speed.

Noteworthy distinct values of  $b$  and  $\xi$  can define different local path trajectories as shown in Fig. 2. The obtained shape of curve is fully related to the personalized driving style. A sporty driving style with high lateral acceleration provides shape ③ while shape ① is for a relaxed driving style (Fig. 1, top panel).

However, the driving comfort is not only associated with the acceleration but also with the acceleration change, namely the jerk. While the lateral acceleration is correctly bounded, the jerk could show non-acceptable limits. For example, as shown in Fig. 2, the lowest bound of the jerk is around  $6 \text{ m.s}^{-3}$  while the comfort criterion mentioned in (Bae et al., 2020) limits it to  $\pm 2 \text{ m.s}^{-3}$ .

The lateral jerk  $Z_{lat}$  must be bounded to minimize a very uncomfortable feeling. Its expression is derived from  $y(x)$  by supposing  $x(t) = v_x t$ :

$$Z_{lat}(t) = \frac{d^3 y}{dt^3} \quad (3)$$

By substituting (1) in (3) and after some mathematical manipulations, the lateral jerk is given by :

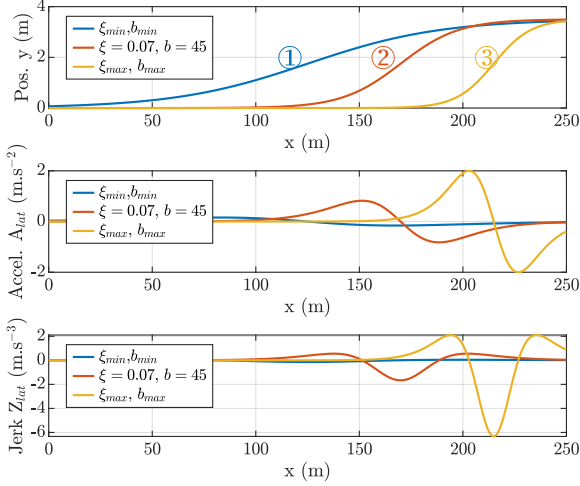


Fig. 2. Sigmoid curves and their derivatives according to the choice of  $\xi$  and  $b$  with  $d_{lat} = 3.5$  m,  $d_{long} = 250$  m,  $v_x = 22$  m.s<sup>-1</sup>,  $a_{ymax} = 2$  m.s<sup>-2</sup> et  $|z_{ymax}| = 2$  m.s<sup>-3</sup>

$$Z_{lat}(t) = d_{lat}(v_x \xi)^3 e^{-\xi(X)} \frac{1 - 4e^{-\xi(X)} + e^{-2\xi(X)}}{(1 + e^{-\xi(X)})^4} \quad (4)$$

with  $X(t) = v_x t - \frac{d_{long}}{2} - b$

As the curve extremums are defined when its derivative is zero, its minimum  $Z_{latmin}$  is obtained for  $X = 0$  allowing to bound  $\xi$ :

$$\xi \leq \xi_{max1} \quad \text{with} \quad \xi_{max1} = \sqrt[3]{\frac{8|Z_{latmin}|}{d_{lat}v_x^3}} \quad (5)$$

So, to fit with both maximal lateral acceleration and jerk, the upper  $\xi$  limit becomes:  $\xi \leq \min(\xi_{max}, \xi_{max1})$ .

Altogether the two parameters  $\xi$  and  $b$  allow modifying the path shape knowing their lower and upper bounds. Our objective is to find the best pair meeting a personalized driving style requirement based on two characteristics relaxed or sporty, as curve ② in Fig. 2, according to the definition of normalized comfort. This could be done by optimizing a cost criterion.

### 3.2 Cost criterion definition

The  $[\xi, b]$  relaxed or sporty characteristics can be defined by a cost criterion introduced hereafter:

- **Smooth/relaxed** driving style can be associated with the acceleration change, i.e. the jerk synonymous with comfort. In our study, since the longitudinal speed is assumed constant during overtaking, only the lateral jerk  $Z_{lat}$  is taken into account. For the local sigmoid path, as shown in (5), the jerk is directly dependent on parameter  $\xi$ . Consequently, a comfortable path is obtained by minimizing  $\xi$  to avoid sharp lane change. To normalize results (comprised between 0 and 1), the proposed cost function is:

$$\begin{cases} J_{smooth} = \min_{\xi} \left( \frac{\xi - \xi_{min}}{\xi_{max} - \xi_{min}} \right)^2 \\ \xi_{min} \leq \xi \leq \xi_{max} \end{cases} \quad (6)$$

- **Tight/sporty** driving style has to generate a racing feeling. This could be done with the minimization of the local trajectories, i.e. minimizing the distance

spent on the adjacent lane. Assuming that  $d_{long}$  is constant, this can be achieved using only the parameter  $b$  in (1). Considering  $b_{max}$  and  $b_{min}$  imposed by safety maneuver constraints (see Section 4), the bounds of the spatial delay  $b$ , and the necessity of a normalized cost criterion, the tight cost criterion is defined as follows:

$$\begin{cases} J_{tight} = \min_b \left( \frac{b_{max} - b}{b_{max} - b_{min}} \right)^2 \\ b_{min} \leq b \leq b_{max} \end{cases} \quad (7)$$

As shown in Fig. 2, the two  $J_{smooth}$  and  $J_{tight}$  cost functions relying on parameters  $\xi$  and  $b$  respectively are antagonistic: sporty style requires a high spatial delay obtained for high curvature form factor while relaxed style requires a low form factor obtained for low spatial delay. A smooth continuous variation from relaxed to sporty S shapes is performed introducing a weighting factor  $\alpha$  between the two cost functions (6) and (7). So, we propose a global cost function  $J$  couple the smooth and tight criteria:

$$\begin{cases} J = (1 - \alpha)J_{smooth} + \alpha J_{tight} \\ 0 \leq \alpha \leq 1 \end{cases} \quad (8)$$

## 4. PERSONALIZED OVERTAKING MANEUVER

Each phase of the overtaking maneuver (see Section 2) requires particular bounds and constraints on the global cost function (8) according to safety and continuity conditions. This section describes how these conditions are considered in the optimization algorithm.

### 4.1 Pullout phase

As shown in Fig. 3,  $t_{end}$  defines the time where EV and LV are side by side and also the pullout phase length  $d_{long}$  because  $d_{long} = x_{EV}(t_{end})$ . Thus:

$$d_{long} = \frac{v_{EV}}{v_{EV} - v_{LV}} x_{LV0} \quad (9)$$

where  $x_{LV0}$  is the initial inter-distance between EV and LV.

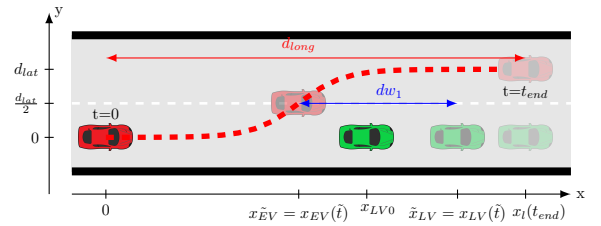


Fig. 3. Pullout phase

The **continuity** constraint ensures a smooth transition between paths. This transition is defined at the local curve extremities, i.e. for  $x_{EV} = 0$ ,  $x_{EV} = d_{long}$  and respectively for lateral position  $y = 0$  and  $y = d_{lat}$  with relative error  $y_{err}$  to tolerate minimum discontinuity. The continuity factor imposes a system of inequalities:

$$\begin{cases} y(0) \leq y_{err} d_{lat} \\ y(d_{long}) \geq (1 - y_{err}) d_{lat} \end{cases} \quad (10)$$

Using (1), system (10) translates into two inequality constraints on  $\xi$  and  $b$ :

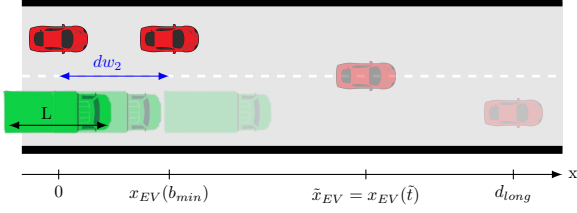


Fig. 4. Return phase : adjacent distance

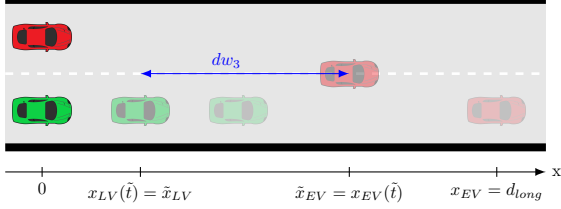


Fig. 5. Return phase : Safety gap

$$\begin{cases} -\xi \left( -b - \frac{d_{long}}{2} \right) \geq \log \left( \frac{1 - y_{err}}{y_{err}} \right) \\ -\xi \left( -b + \frac{d_{long}}{2} \right) \leq -\log \left( \frac{1 - y_{err}}{y_{err}} \right) \end{cases} \quad (11)$$

The longitudinal **safety** gap  $dw_1$  between the two vehicles is defined as the distance between the two vehicles when EV crosses the center line (see Fig. 3). The safety constraint is then given by:

$$\tilde{x}_{LV} - \tilde{x}_{EV} \geq dw_1 \quad (12)$$

where  $\tilde{x}_i$  is the vehicle position when EV crosses the center line. From (12) and (9), the upper bound of parameter  $b$  is given by:

$$b \leq \frac{v_{EV}}{v_{EV} - v_{LV}} \left( \frac{x_{LV0}}{2} - dw_1 \right) \quad (13)$$

Since the lower bound of  $\xi$  is obtained for  $b = 0$  and there is no reason to anticipate a lane change, i.e. for  $b < 0$ , we adopt 0 as its lower bound:

$$b \geq 0 \quad (14)$$

Altogether, the formulation of **pullout phase optimization** is defined by the following cost function, bounds and nonlinear inequalities:

$$\begin{cases} J(\xi, b) = (1 - \alpha) \left( \frac{\xi - \xi_{min}}{\xi_{max} - \xi_{min}} \right)^2 + \alpha \left( \frac{b_{max} - b}{b_{max} - b_{min}} \right)^2 \\ 0 \leq \alpha \leq 1 \\ \xi_{min} \leq \xi \leq \xi_{max} \\ 0 \leq b \leq b_{max} \\ -\xi \left( -b - \frac{d_{long}}{2} \right) \geq \log \left( \frac{1 - y_{err}}{y_{err}} \right) \\ -\xi \left( -b + \frac{d_{long}}{2} \right) \leq -\log \left( \frac{1 - y_{err}}{y_{err}} \right) \end{cases} \quad (15)$$

#### 4.2 Return phase

To minimize path segment connection, phases ② and ③ of the overtaking maneuver (see Fig. 1) are fused. The side by side driving phase is obtained by a distance  $dw_2$  where EV drives along LV as shown in Fig. 4 such that:

$$dw_2 = \frac{v_{EV}}{v_{EV} - v_{LV}} L, \quad (16)$$

where  $L$  is the LV length.

A safety gap is maintained between both vehicles. Following the same approach as in the pullout phase,  $dw_3$  defines the vehicle inter distance to be respected by EV when it crosses back the center line (see Fig. 5). The parameter  $d_{long}$  gives the maximal distance for the return maneuver.

Same requirements are used to define the cost function bounds and constraints. Like (11), the **continuity** factor is given by:

$$\begin{cases} y(d_{long}) \leq y_{err} d_{lat} \\ y(dw_2) \geq (1 - y_{err}) d_{lat} \end{cases} \quad (17)$$

Using (1), the following inequality constraints are obtained:

$$\begin{cases} -\xi \left( dw_2 - b - \frac{d_{long}}{2} \right) \geq \log \left( \frac{1 - y_{err}}{y_{err}} \right) \\ -\xi \left( -b + \frac{d_{long}}{2} \right) \leq -\log \left( \frac{1 - y_{err}}{y_{err}} \right) \end{cases} \quad (18)$$

Therefore, the **safety** constraint becomes:

$$\tilde{x}_{EV} - \tilde{x}_{LV} \geq dw_3 \Rightarrow b \geq dw_3 \frac{v_{EV}}{v_{EV} - v_{LV}} - \frac{d_{long}}{2} \quad (19)$$

and with the maximum curvature, continuity has to be maintained with  $b$  upper bound:

$$b \leq \frac{d_{long}}{2} - \frac{1}{\xi_{max}} \log \left( \frac{1 - y_{err}}{y_{err}} \right) \quad (20)$$

Altogether, the formulation of the **return phase optimization** is defined by the following cost function, bounds, and nonlinear inequalities:

$$\begin{cases} J(\xi, b) = (1 - \alpha) \left( \frac{\xi - \xi_{min}}{\xi_{max} - \xi_{min}} \right)^2 + \alpha \left( \frac{b - b_{min}}{b_{min} - b_{max}} \right)^2 \\ 0 \leq \alpha \leq 1 \\ \xi_{min} \leq \xi \leq \xi_{max} \\ b_{min} \leq b \leq b_{max} \\ -\xi \left( dw_2 - b - \frac{d_{long}}{2} \right) \geq \log \left( \frac{1 - y_{err}}{y_{err}} \right) \\ -\xi \left( -b + \frac{d_{long}}{2} \right) \leq -\log \left( \frac{1 - y_{err}}{y_{err}} \right) \end{cases} \quad (21)$$

## 5. VALIDATION RESULTS

In the first step of the validation process, a proof of concept is performed. Both optimization formula (15) and (21) together with criterion (8) are tested to modify the sigmoid parameters to switch the driving feeling from comfortable to sporty. In the second step, the optimization algorithm is integrated into a simulation architecture allowing to generate a local path for overtaking maneuvers and validates dynamically EV trajectories.

### 5.1 Optimization findings

To observe the evolution of  $\xi$  and  $b$  for a driving style switching from relaxed to sporty, both pullout and return optimization processes (15) and (21) are computed under MATLAB software using `fmincon` function with the interior-point solver algorithm. Since both cost functions

are convex, they offer a global solution regardless of the different constraints.

We adopt the conventional  $2.v_{EV}$  distance for the safety gap  $dw_1$  where 2 s is the global reaction time. There is no legal definition for the safety distance  $dw_3$ , so we adopt  $dw_3 = 25$  m. Since there is no constraint on the return maneuver length,  $d_{long}$  is fixed to  $dw_2 + 200$  m where 200 m could correspond to a maximal distance for a lidar to detect another leader vehicle. This sensor characteristic is used to set  $x_{LV0} = 200$  m. If LV is a truck, the length L is chosen to be 20 m while L of is set to 5m for a car. Road width lane  $d_{lat}$  is set to 3.5 m.

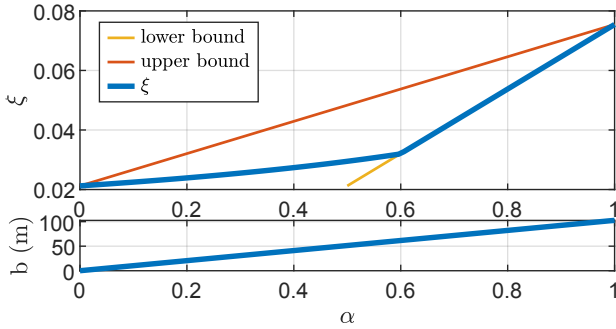


Fig. 6. Variations of sigmoid parameters with driving style during pullout phase

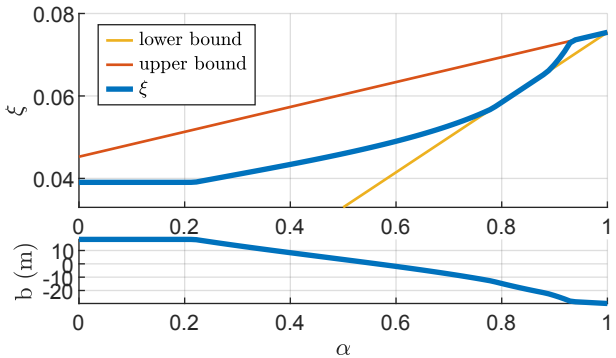


Fig. 7. Variations of sigmoid parameters with driving style during return phase

Parameter  $\alpha$  varying from 0 to 1 allows an evolution for a driving style going from relaxed to sporty. Raw optimization computational results present a very steep slope and can not be directly used. In both cases, the full-scale  $\xi$  and  $b$  variations are obtained by defining an operating area with inequality constraints bounded by line segments as shown in Fig. 6 and 7. For the pullout phase, the inequalities are:

$$\begin{cases} \xi < (\xi_{max} - \xi_{min})\alpha + \xi_{min} \\ \xi > 2(\xi_{max} - \xi_{min})(\alpha - 0.5) + \xi_{min} \\ b < \alpha b_{max} \end{cases} \quad (22)$$

and for the return phase, inequalities are related to parameter  $\xi$  only:

$$\begin{cases} \xi < (\xi_{max} - 0.6\xi_{max})\alpha + 0.6\xi_{max} \\ \xi > 2(\xi_{max} - \xi_{min})(\alpha - 0.5) + \xi_{min} \end{cases} \quad (23)$$

With those new constraints, optimization findings are in line with expectations on both continuity and the

monotony. In both phases, the higher the parameter  $\alpha$  is, the higher the  $\xi$  is, generating higher lateral acceleration and consequently sporty feeling. Moreover, this feeling is emphasized by a decreasing gap between the vehicles when a sporty driving style is required. In phase ① in Fig. 1,  $b$  should be positive, whereas in phase ③ it should be negative.

The initial vehicle inter-distance or global return distance depends on the driving situation and is not necessarily equal to 200 m. It is interesting to note in Fig. 8 that  $\xi$  and  $b$  maintain their relative properties depending on driving style: with a sporty style,  $\xi$  remains high regardless of distances and imposes a higher the curvature form and a lower safety gap. On the opposite, with comfortable style,  $b$  remains low regardless of  $x_{LV0}$  providing low  $\xi$  and smooth trajectory. With a daily style (an intermediate driving style defined by  $\alpha = 0.5$ ), the optimization adjusts both parameters in relation to safety distance when  $d_{long}$  is short in the return phase. The same conclusions are obtained for the return phase.

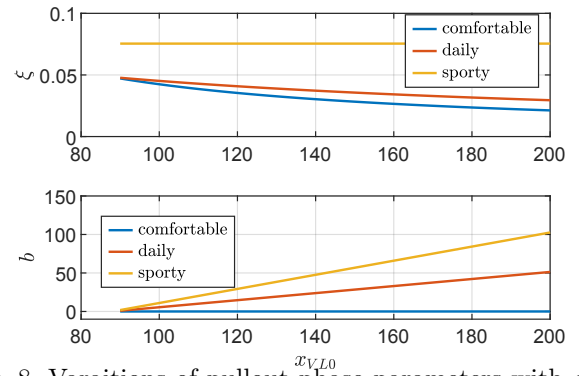


Fig. 8. Variations of pullout phase parameters with  $x_{LV0}$  value

## 5.2 Driving situations

The validation is performed by integrating the parameters optimization algorithm in a local path generation to simulate a realistic overtaking scenario. We perform simulations on a 1000 m distance straight line. There are two lanes, each one is 3.5 m large without static or dynamic obstacles (except LV). EV starts at position (0,0) at 300 m behind LV. The leader is either a car (5 m long) or a truck (20 m long). The ego speed is  $22 \text{ m.s}^{-1}$  and the leader speed is  $10 \text{ m.s}^{-1}$ . EV detects LV when 200 m behind it. Demonstration is done for 3 different driving styles corresponding to 3 values of  $\alpha$ : 0-comfortable, 0.5-daily and 1-sporty.

## 5.3 Results and discussion

Fig. 9 and 10 compare trajectories with the different driving styles. Pullout and return trajectories are similar independently of the vehicle type. However, we can notice that the distance covered on the adjacent lane for truck overtaking is longer than when overtaking a car due to its length.

Acceleration and jerk do not exceed the fixed limits (respectively  $\pm 2 \text{ m.s}^{-2}$  and  $\pm 2 \text{ m.s}^{-3}$ ) and are conform

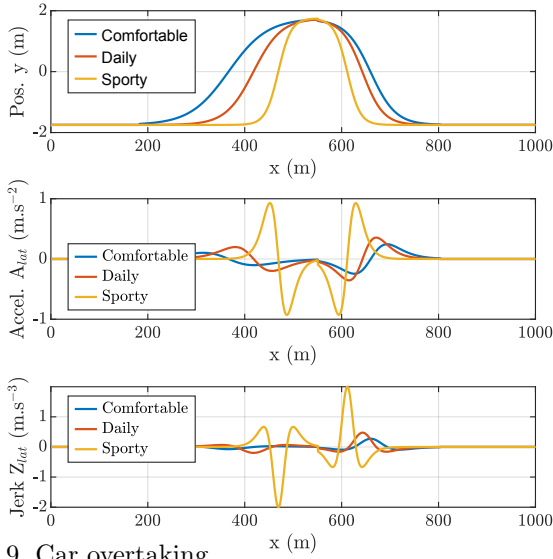


Fig. 9. Car overtaking

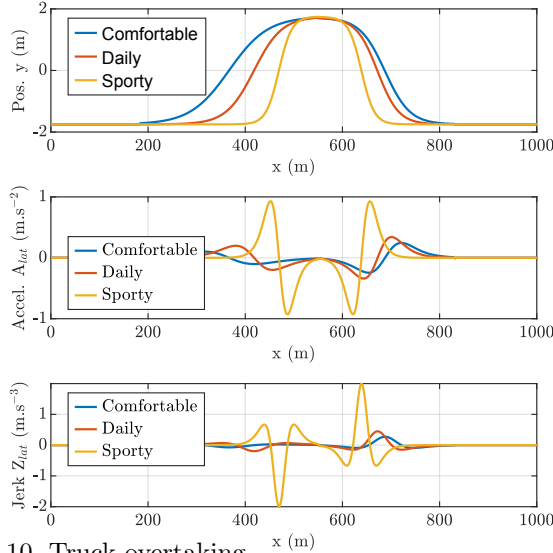


Fig. 10. Truck overtaking

to the driving style. The sporty driving experience is reinforced when the vehicle gap decreases. In addition, comfort is reduced for the return phase due to a small distance  $d_{long}$  set at 200 m. Improvement could be done by adjusting this parameter to  $\alpha$ .

Fig. 11 shows the truck overtaking maneuver with a sporty driving style. The circle markers give ego and leader positions when ego crosses center line. Both safety gaps are  $dw_1 = 44 \text{ m} \geq 2v_{EV}$  and  $dw_3 = 48 \text{ m} \geq 25 \text{ m}$  highlighting that safety constraints are respected.

## 6. CONCLUSION AND PERSPECTIVES

In this work, we have optimized the parameters of a sigmoid function to personalize local trajectory in an overtaking maneuver according to a driving style preference. This optimization is performed by introducing continuity and safety constraints. A variation shape from smooth to tight can be obtained only by controlling a single parameter  $\alpha$  in order to personalize driving style. A simulation

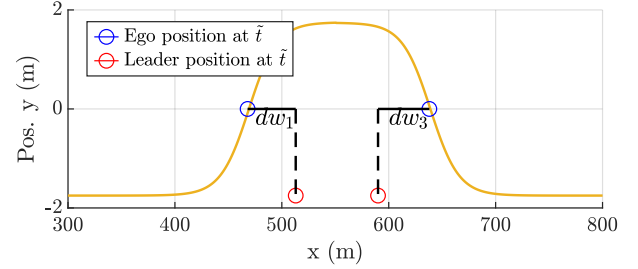


Fig. 11. Safety gap

framework is presented to confirm our analysis. Future work is considered to extend it to personalized decision making by relaxing some assumptions.

## REFERENCES

- Alia, C., Gilles, T., Reine, T., and Ali, C. (2015). Local trajectory planning and tracking of autonomous vehicles, using clothoid tentacles method. In *2015 IEEE Intelligent Vehicles Symposium (IV)*, 674–679. IEEE, Seoul, South Korea.
- Ammour, M., Orjuela, R., and Basset, M. (2020). Trajectory Reference Generation and Guidance Control for Autonomous Vehicle Lane Change Maneuver. In *2020 IEEE 28th Mediterranean Conference on Control and Automation (MED)*, 13–18. Saint-Raphaël, France.
- Bae, I., Moon, J., Jhung, J., Suk, H., Kim, T., Park, H., Cha, J., Kim, J., Kim, D., and Kim, S. (2020). Self-Driving like a Human driver instead of a Robocar: Personalized comfortable driving experience for autonomous vehicles. In *2019 Conference on Neural Information Processing Systems (NeurIPS)*. Vancouver, Canada.
- Ben-Messaoud, W., Basset, M., Lauffenburger, J.P., and Orjuela, R. (2018). Smooth Obstacle Avoidance Path Planning for Autonomous Vehicles. In *2018 IEEE International Conference on Vehicular Electronics and Safety (ICVES)*, 1–6. Madrid, Spain.
- Claussmann, L., Revilloud, M., Gruyer, D., and Glaser, S. (2020). A Review of Motion Planning for Highway Autonomous Driving. *IEEE Transactions on Intelligent Transportation Systems*, 21, 1826–1848.
- Gonzalez, D., Perez, J., Milanés, V., and Nashashibi, F. (2016). A Review of Motion Planning Techniques for Automated Vehicles. *IEEE Transactions on Intelligent Transportation Systems*, 17, 1135–1145.
- González, D., Milanés, V., Pérez, J., and Nashashibi, F. (2016). Speed profile generation based on quintic bézier curves for enhanced passenger comfort. In *2016 IEEE 19th International Conference on Intelligent Transportation Systems (ITSC)*, 814–819. Rio de Janeiro, Brazil.
- Huang, C., Lv, C., Hang, P., and Xing, Y. (2021). Toward Safe and Personalized Autonomous Driving: Decision-Making and Motion Control With DPF and CDT Techniques. *IEEE/ASME Transactions on Mechatronics*, 26, 611–620.
- Rajamani, R. (2012). *Vehicle Dynamics and Control*. Mechanical Engineering Series. Springer US, Boston, MA.